Continental-Scale River Flow in Climate Models

JAMES R. MILLER

Department of Marine and Coastal Sciences, Cook College, Rutgers University, New Brunswick, New Jersey

GARY L. RUSSELL

NASA/Goddard Space Flight Center, Institute for Space Studies, New York, New York

GUILHERME CALIRI

Hughes STX Corporation, New York, New York

(Manuscript received 25 January 1993, in final form 12 October 1993)

ABSTRACT

The hydrologic cycle is a major part of the global climate system. There is an atmospheric flux of water from the ocean surface to the continents. The cycle is closed by return flow in rivers. In this paper a river routing model is developed to use with grid box climate models for the whole earth. The routing model needs an algorithm for the river mass flow and a river direction file, which has been compiled for 4° × 5° and 2° × 2.5° resolutions. River basins are defined by the direction files. The river flow leaving each grid box depends on river and lake mass, downstream distance, and an effective flow speed that depends on topography. As input the routing model uses monthly land source runoff from a 5-yr simulation of the NASA/GISS atmospheric climate model (Hansen et al.). The land source runoff from the 4° × 5° resolution model is quartered onto a 2° × 2.5° grid, and the effect of grid resolution is examined. Monthly flow at the mouth of the world's major rivers is compared with observations, and a global error function for river flow is used to evaluate the routing model and its sensitivity to physical parameters. Three basinwide parameters are introduced: the river length weighted by source runoff, the turnover rate, and the basinwide speed. Although the values of these parameters depend on the resolution at which the rivers are defined, the values should converge as the grid resolution becomes finer. When the routing scheme described here is coupled with a climate model's source runoff, it provides the basis for closing the hydrologic cycle in coupled atmosphere–ocean models by realistically allowing water to return to the ocean at the correct location and with the proper magnitude and timing.

1. Introduction

Rivers are a major component of the earth's hydrologic cycle. Although at any given time rivers hold only a small fraction of the world's total water, they provide the critical link for returning water from continents to the ocean. This long-term global water budget has been discussed in several papers (Baumgartner and Reichel 1975; Korzoun et al. 1977; Milliman and Meade 1983; Russell and Miller 1990).

Since global climate models usually neglect the transport of water back to the ocean by rivers, they do not have a closed hydrologic cycle. The scales of these models are much larger than the catchment basin scales at which most hydrologists work. This paper introduces a routing model that uses land source runoff from each grid box of a global climate model to calculate river flow and thus to return water to the ocean with the proper location and timing.

The inclusion of river flow in climate models is important for several reasons. One is that it provides an excellent method for climate modelers to examine their hydrology schemes because their model's river flow can be compared with observed gauging stations. Observed river flow provides a better diagnostic than observed grid-box runoff, which is not measured directly. A second reason is that river flow provides freshwater to the ocean, which affects both ocean convection and circulation in atmosphere–ocean models. Mysak et al. (1990) suggest that salinity anomalies in the North Atlantic Ocean, which could affect the thermohaline circulation, are related to ice transport through the Fram Strait, which in turn may be related to anomalous river flow into the Arctic Ocean.

There are several different components of runoff that are used in this paper. Surface runoff is the precipitation or snow melt that does not infiltrate into the ground, but that reaches a river or lake within a few days of falling or melting. Groundwater runoff is water that

Corresponding author address: Dr. James R. Miller, Institute of Marine and Coastal Sciences, Cook College, Rutgers University, P.O. Box 231, New Brunswick, NJ 08903-0231.

infiltrates into the ground to the water table and moves laterally to a river or lake. Land source runoff is the sum of surface and groundwater runoff. Source runoff within a grid box is the sum of land source runoff and the net flux of precipitation minus evaporation directly onto the river and lake surfaces. After water reaches a river or lake, it moves downstream and is referred to as river flow. In this paper, the word runoff refers to water that is moving toward a river or lake, and the word flow refers to the movement of water that is in a river or lake.

For individual river basins, source runoff depends on precipitation and evaporation within the basin, and the ability of the land to store water in the soil or above it as snow. Water storage in the ground depends on soil type, depth, and heterogeneity and on the seasonally varying vegetation. River flow at the mouth depends on source runoff, basin topography, and the characteristics of the river channel.

In this paper, the source runoff from each grid box of an atmospheric general circulation model is used to calculate the monthly flow at the mouths of the world's major rivers. In the river routing model, the magnitude and timing of river flow depend on the choice of the local effective flow speed, which may depend on the topography gradient. Sensitivity of the flow at the river mouth to this local effective flow speed is discussed.

2. The atmospheric model

The atmospheric general circulation model (GCM) of the NASA/Goddard Institute for Space Studies (Hansen et al. 1983) is used in this study. The model includes a two-layer hydrologic model. A brief description of the model is given here. The GCM has a horizontal resolution of 4° latitude by 5° longitude and nine vertical layers. The fluid dynamic equations are solved numerically conserving mass, momentum, total energy, and water vapor. The GCM also includes source terms for momentum, heat, and water vapor due to processes such as surface interaction, radiation, and condensation. At the surface, grid boxes are divided into land and ocean fractions. The continental topography is averaged from the National Geophysical Data Center (1988) 5-min resolution.

The land source runoff in each grid box depends on the precipitation, evapotranspiration, and water storage within the land portion of the grid box. The evapotranspiration E (kg m^{-2} s^{-1}) is calculated as the product

$$E = \beta \rho C V (q_G - q_S), \quad (1)$$

where β is a dimensionless efficiency factor for evapotranspiration, ρ (kg m^{-3}) is the surface air density, C is a dimensionless drag coefficient that depends on stability, V (m s^{-1}) is the surface wind speed, q_G is the saturation specific humidity defined by the ground temperature and surface pressure, and q_S is the surface air specific humidity at 10 m above the surface. The GCM's precipitation is compared with observations in Russell and Miller (1990).

The annual changes in soil-moisture storage are negligible compared to annual precipitation, evapotranspiration, and land source runoff, but during each time step, the amount of storage directly affects both β and the runoff. The GCM has a two-layer soil-moisture storage scheme described in Hansen et al. (1983). The upper layer responds hourly to evapotranspiration and precipitation, and the lower layer acts as a seasonal reservoir. There is a 2-day time constant for diffusion of water between the two layers, except during the growing season when the upward diffusion occurs instantly over vegetated areas. In the GCM, the water field capacities of the two layers do not depend on soil characteristics, but do depend on the vegetation characteristics of each grid box, which were taken from Matthews (1983).

During a time step Δt in which precipitation falls or snow melts, excess water that does not infiltrate into the ground runs off from the grid box. The land source runoff, R, is generated during that time step and is given by

$$R\,(\text{kg}) = \max\left[\frac{1}{2}(P + N)\Delta t W/W_c,\ (P + N)\Delta t + W - W_c\right], \quad (2)$$

where P (kg s^{-1}) is the precipitation rate, N (kg s^{-1}) is the rate of snowmelt, W (kg) is the water and ice in the first layer, and W_c (kg) is the water field capacity. The factor β in (1) is equal to W/W_c unless the ground is snow covered in which case $\beta = 1$. The coefficient of one-half in (2) was chosen so that the computed summer temperatures would be consistent with observations (Hansen et al. 1983).

Hydrologists model surface and groundwater runoff separately. In the GCM, the parameterization given by (2) makes no distinction between surface and groundwater runoff that leaves the land, and in addition, there is no time delay for excess precipitation or snowmelt to reach the rivers or lakes of a grid box. Probst and Sigha (1989) have done the apportionment between surface and groundwater runoff for the world's major rivers, and the impact of doing this in the river routing model is discussed later. A more physically based model that calculates groundwater has been developed by Abramopoulos et al. (1988) and will be used in future simulations. Their model addresses the time lag between the availability of excess precipitation or snowmelt and when it reaches the river and lake system within a grid box.

The land source runoff is based on monthly averages from the last five years of a six-year GCM simulation. During a time step Δt, land source runoff is added to the mass of the river and lake systems within each grid

box. Water can be removed thereafter by evaporation or added by precipitation directly onto the river and lake surface. This water combined with the land source runoff is called source runoff,

$$S = R + (P_L - E_L)\Delta t, \tag{3}$$

where P_L and E_L (kg s^{-1}) are the precipitation and evaporation rates over the area covered by rivers or lakes.

In the remainder of this paper, P_L and E_L are assumed to be zero, and the source runoff is equal to the land source runoff (i.e., $S = R$). We have done several cases in which P_L and E_L are not zero, and for most rivers, the flow at the river mouth is insignificantly different than when they are zero. There are several reasons for assuming $S = R$ in this paper. The first reason is that the temperature of water in the river and lake system is not calculated from physical principles but is based on a crude climatology of lake temperatures. Evaporation from rivers and lakes depends critically on water temperatures. A second reason is that individual grid boxes can act as sinks of water if lake evaporation exceeds the sum of the inputs from land source runoff, river flow, and precipitation onto the lake. Although this does happen in real river systems and causes the surface area of the water body to change, the surface area of rivers and lakes is fixed in the GCM. For these reasons, P_L and E_L are assumed to be 0 in this paper.

Each of the climate model's 4° × 5° grid boxes has been quartered so that river basins can be defined at 2° × 2.5° resolution. The land source runoff calculated by the GCM is assumed to be evenly distributed proportional to the land area over the continental grid boxes of the finer grid. In the remainder of this paper, references to the river and lake systems will be to the 2° × 2.5° resolution unless otherwise noted.

Wood et al. (1992) have described a statistical approach to represent the land surface hydrology in GCMs. Their water balance model statistically represents the infiltration capacity within a GCM grid box. They found that their method produced better short-term variability of land source runoff within a model grid box than bucket models. More realistic distributions of subgrid hydrologic processes could be obtained by using probability density functions for the spatial distribution of precipitation in atmospheric models as discussed by Entekhabi and Eagleson (1989). Although the land source runoff in this paper is based on the deterministic formulation of (2), statistical distributions may be used with the routing model developed here.

3. The river direction files

The accurate simulation of source runoff within a river basin is only one step in calculating monthly flow at the river's mouth. There must be directed paths connecting grid boxes near a river's headwaters to grid boxes that are successively closer to its mouth. Then, there must be a way to specify how fast water moves from a grid box to its downstream neighbor.

Two separate river direction files were created, one for 4° × 5° horizontal resolution and one for 2° × 2.5° resolution. The international date line and the equator are grid-box edges for both resolutions so that each 4° × 5° grid box exactly overlays four 2° × 2.5° boxes except at the poles. Figure 1 shows the river direction file for the 2° × 2.5° resolution. Both files are available from the authors.

The river direction files are based on world maps (Korzoun et al. 1977; Times of London 1967). Care was taken to assure that if a grid box primarily drains through a particular channel of a river on the earth, then the direction files would move the grid box's source runoff to that channel and not divert it to another river basin or to a different tributary of the same river. The direction files are not seasonally dependent, and directions are assigned to grid boxes in which flow occurs only in some seasons. If there is no arrow in a grid box, any source runoff generated is assumed to drain internally and not reach the ocean. Such grid boxes are usually deserts. Directions over Greenland and Antarctica were based solely on the topography gradient. River directions for the profusion of islands in northern Canada are somewhat arbitrary.

As one moves downstream from a river's headwaters to its mouth, the flow generated by the model increases. If the monthly source runoff, S, is the same every year, the total annual mass flow at any location will be equal to the sum of monthly source runoff that is upstream of the location. Figure 2 shows the equilibrium annual water flow from each of the climate model's quartered grid boxes. This flow does not depend on local effective flow speeds. The figure shows that the water flow increases toward the river mouth, and it also indicates where the source runoff originates. If the arrows are large throughout the basin, as they are for the Nile River, the bulk of the source runoff originates far upstream. Otherwise, the flow builds gradually toward the mouth as more water is added to the river.

4. River routing model

The rate at which water leaves a grid box depends on many factors, including the river mass M (kg) above the sill depth, the mean distance d (m) between the grid box and its downstream neighbor, and the downstream topography gradient. The river moves water from a grid box to its downstream neighbor according to the equation

$$F(\text{kg s}^{-1}) = M \cdot u/d, \tag{4}$$

where u (m s^{-1}) is an effective flow speed of water from a grid box to its downstream neighbor. The value of u depends on local characteristics of the river basin, such as its morphology and topography gradient. In

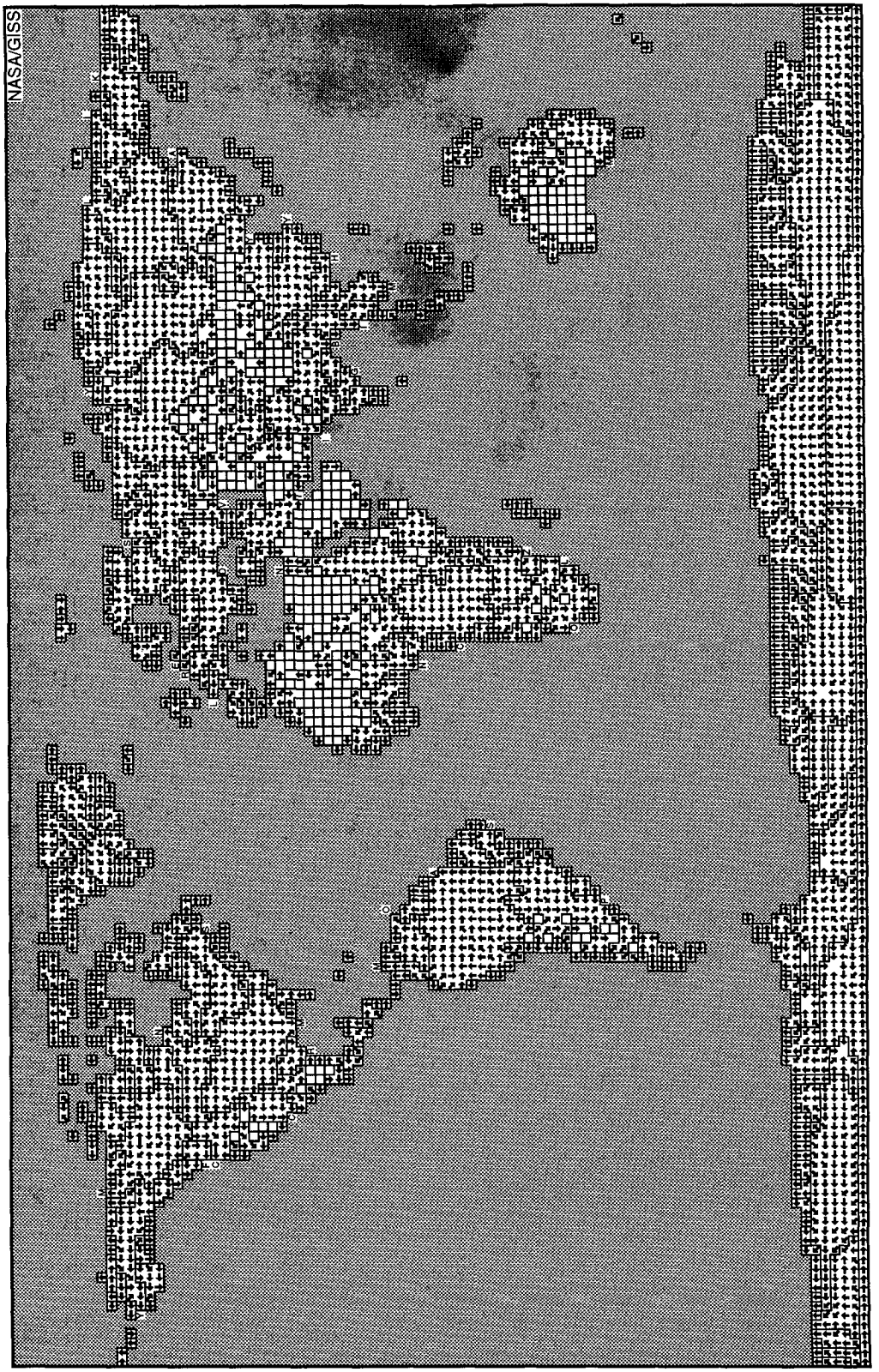

FIG. 1. Direction map for river flow for 2° × 2.5° horizontal grid resolution. Arrows indicate the direction of flow out of a grid box. Boxes without arrows drain internally. A letter corresponding to the first letter of each river's name is located at the river's mouth.

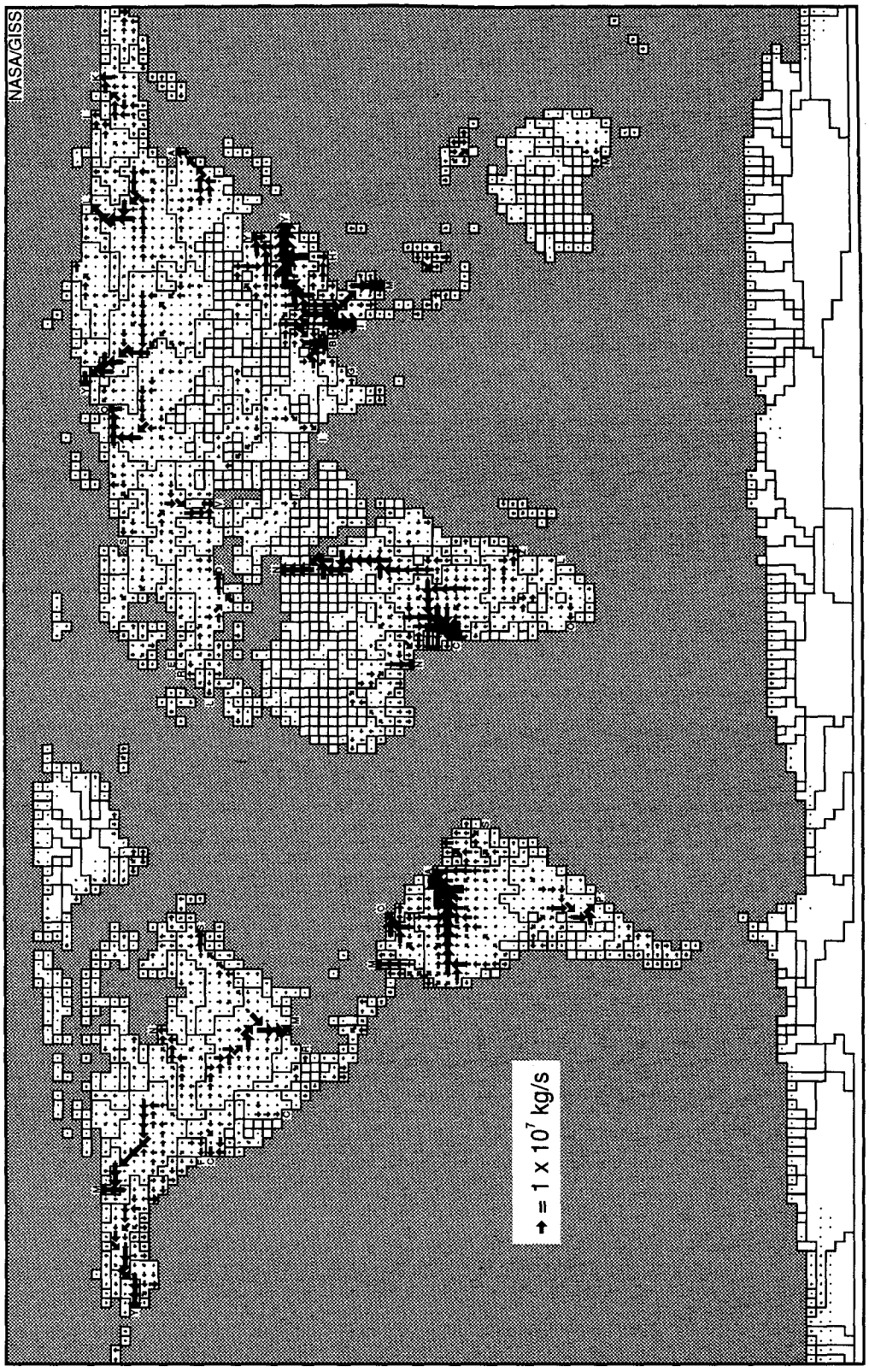

FIG. 2. Total annual river mass flux for the 2° × 2.5° grid boxes. The area of an arrow is proportional to the mass flux out of a grid box. A letter corresponding to the first letter of each river's name is located at the river's mouth.

this paper, u is either a global constant or u depends on the downstream topography gradient. The latter choice is discussed in section 6.

Equation (4) can be put into a more familiar form if we let $M = \rho V$, where ρ is the water density and V is the volume of water in a grid box. For a river flowing in a channel with a uniform cross-sectional area A, the volume can be written as $V = A\,d$, and (4) is equivalent to

$$F = \rho A u. \quad (5)$$

Equation (5) is the common form for expressing the flux across an interface between two grid boxes.

The river mass, M, includes both river water and lake water above the sill depth. The sill depth is the depth below which water cannot flow out of a grid box. For rivers we assume the sill depth is the bottom of the river and that outflow always occurs when the river mass is greater than zero. For lakes a sill depth must be specified, and if the water level in that grid box falls below the sill depth, there is no flow out of the grid box. If M becomes negative because evaporation has caused the river or lake level to drop below the sill depth, then F is set to zero.

Equation (4) is the basis for a continuous streamflow model. A common formulation forces the product u/d to be a constant (Linsley et al. 1982; Singh 1989). If $\omega\,(s^{-1}) = u/d$ is taken as a constant rate coefficient, then $F = \omega M$. Vorosmarty et al. (1989) have used this formulation in a routing scheme for the Amazon River at 0.5° resolution. The formulation $F = \omega M$ is valid if the distance from a grid box to its downstream neighbor is constant throughout the domain, which is the case for a square grid domain where the flow is either north–south or east–west. In our global model, the use of a constant ω is invalid for three reasons: our grid boxes are not square, downstream flow can occur to diagonally adjoining grid boxes, and the east–west widths of grid boxes change with latitude because of the convergence of meridians toward the poles in the GCM grid. Another problem in using a constant ω is that it depends on grid resolution. For these reasons we use the more general formulation given by (4) in which the downstream distance d depends on resolution, direction, and latitude.

Equation (4) is used as the basis for the routing model used in this paper. During a time step, the change in lake and river mass in a grid box is given by

$$M(t + \Delta t) - M(t) = S + \Delta t \Sigma F_{IN} - \Delta t F_{OUT}, \quad (6)$$

where F_{OUT} is the rate at which river mass leaves a grid box, ΣF_{IN} is the river mass entering, and S is the source runoff defined by (2) and (3). The summation before F_{IN} occurs because each grid box may receive river mass from several upstream boxes, but there is at most one outlet.

Figures 3a–5a show the monthly flow at the mouth of the Congo (Zaire), Mississippi, and Yenesei

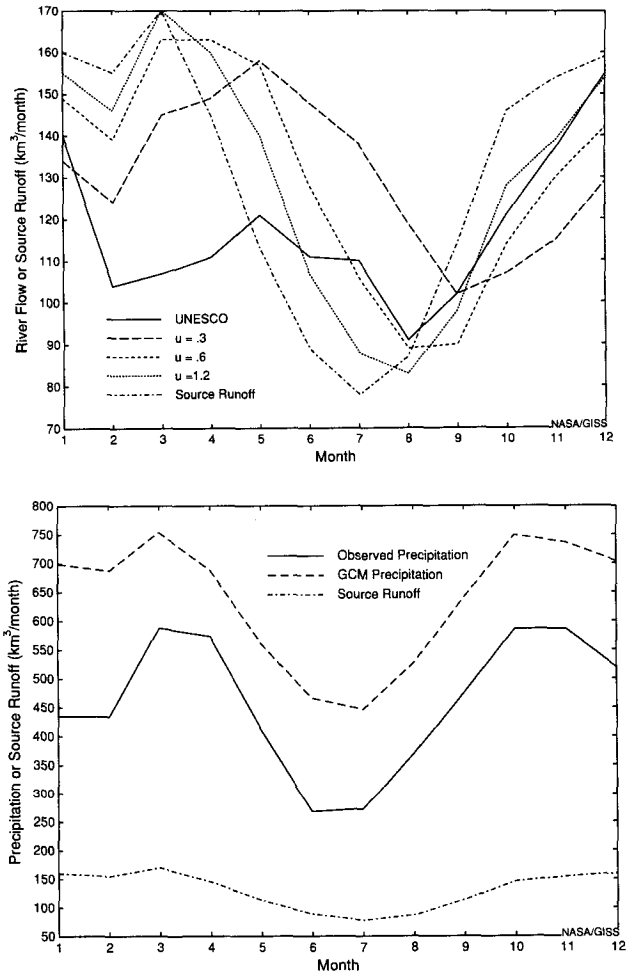

FIG. 3. (a) Monthly river flow at the mouth of the Congo (Zaire) River for three globally uniform effective flow speeds of $u = 0.3, 0.6, 1.2$ m s^{-1}. The observed river flow is from UNESCO. (b) The monthly basinwide precipitation for the GCM compared with the observations of Legates and Willmott (1990). The source runoff is shown for comparison in both (a) and (b).

Rivers for three different globally constant effective flow speeds: $u = 0.3$, 0.6, and 1.2 m s^{-1}. Also shown in the figures is the source runoff integrated over the basin and the United Nations Educational, Scientific, and Cultural Organization (UNESCO) observed river flow at the station nearest to the mouth. Kuhl and Miller (1992) examined the monthly variation of source runoff for 16 of the rivers in this study. Figures 3b–5b show the corresponding monthly precipitation. The source runoff is included in both the (a) and (b) figures to show its relationship to basinwide precipitation and river flow at the mouth and to show the difference in scales. As u decreases, water moves more slowly through the basin, and the flow at the mouth becomes more evenly distributed throughout the year. As u increases, flow at the mouth more closely coincides with the source runoff. If u were increased without limit,

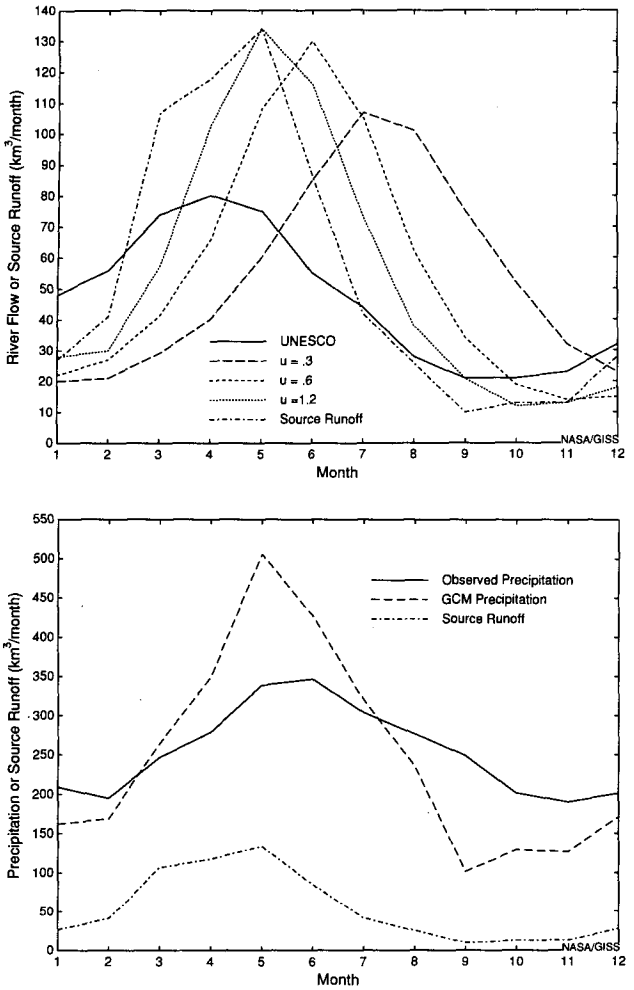

FIG. 4. The Mississippi River. Otherwise the same as Fig. 3.

the source runoff and the river flow at the mouth would converge.

Figures 3b–5b show that for the Congo, Mississippi, and Yenesei River basins, the GCM simulates the annual phase of precipitation well but generates too much precipitation in the spring for the Mississippi and Yenesei. For the Congo the GCM's precipitation is uniformly too large, but the timing of the minimum precipitation in June and July is well simulated. The observed flow at the mouth has maxima in December and May for the Congo. The model attains a maximum in May when $u = 0.3$ m s^{-1}. For the Mississippi River, none of the three effective flow speeds produces monthly flow at the mouth in phase with the observed. Van Blarcum (1992) showed that this is largely because the GCM produces too much precipitation and land source runoff in the western part of the basin (Missouri River) and too little in the eastern part (Ohio River).

The Yenesei River in northern Asia is typical of most high-latitude river basins. The flow at the mouth is maximum in the spring when snow melts. The model's ability to reproduce the magnitude and timing of the peak flow depends on the ability to accumulate snow during the winter season, to calculate temperatures so that snowmelt occurs at the right time, and to route water through the river at the proper speed. The model captures this event best at the intermediate speed ($u = 0.6$ m s^{-1}). An interesting feature of this basin is that the source runoff maximum occurs before the precipitation maximum. This is because the late fall and winter precipitation falls as snow that accumulates during the winter. When it melts in the spring, it is available as source runoff.

5. Basinwide turnover rate, river length, and speed

Since climate models can be run at different resolutions and with different parameterizations of physical processes, it is useful to define parameters from different model simulations that can be compared. Such a parameter should converge to a finite limit as the resolution becomes finer. In this section we define such

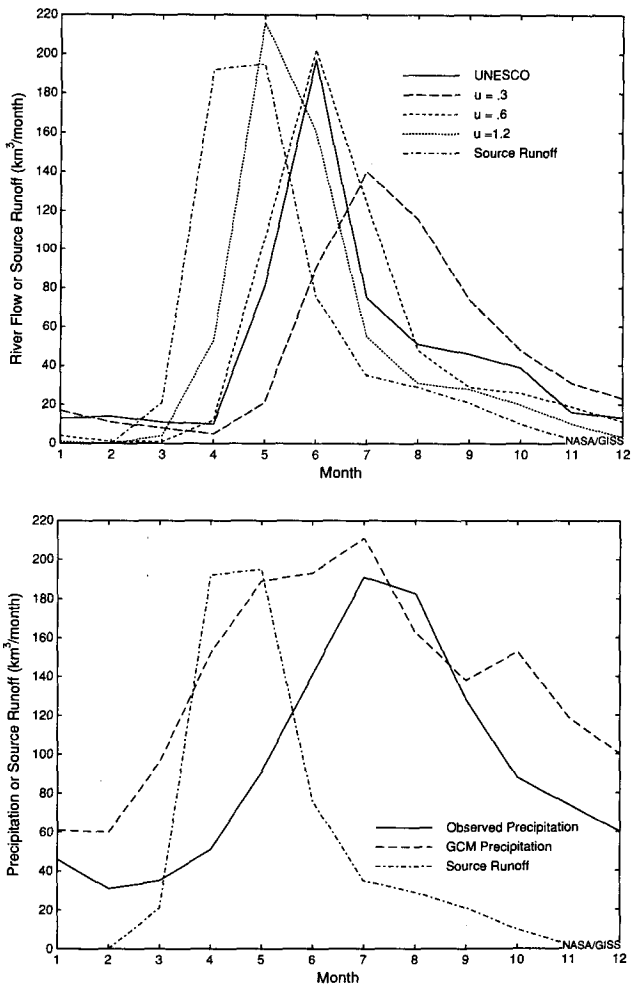

FIG. 5. The Yenesei River. Otherwise the same as Fig. 3.

basinwide parameters for comparing river flow among different model simulations.

One basinwide flow parameter is the mean annual turnover rate for an entire river basin, which is defined as

$$\Omega\ (\mathrm{yr}^{-1}) = \bar{F}_{\mathrm{MOUTH}}/\Sigma\bar{M}, \qquad (7)$$

where $\bar{F}_{\mathrm{MOUTH}}$ is the mean annual mass flow at the river mouth, and $\bar{M}$ is the mean annual river mass above the sill depth with the summation taken over all grid boxes within a river basin. The overbar indicates an annual integral or an annual mean. The value of Ω depends on the formulation for the local effective flow speed, u, in the river routing model.

For each grid box we let λ be the river length from a grid box to the river mouth (i.e., $\lambda = \Sigma d$ along the river path from the grid box to the mouth). A basinwide river length Λ is defined by weighting the length λ with the annual source runoff, $\bar{S}$, to obtain

$$\Lambda = \Sigma\bar{S}\lambda/\Sigma\bar{S}, \qquad (8)$$

where the summations are taken over all grid boxes in the river basin. If all the source runoff had its origin in the same grid box, then Λ would be the value of λ for that grid box. The length Λ depends on the source runoff and the direction file but is independent of the effective flow speed used in the river routing model.

The basinwide turnover rate Ω and the basinwide river length weighted by source runoff Λ are multiplied together to define a third basinwide parameter U defined as

$$U = \Omega\Lambda, \qquad (9)$$

where U represents a basinwide speed. When u in (4) is a global constant, then $u = U$. Although this result is difficult to derive, it can be obtained by substituting (4) into (6) with u held constant and then summing over the river path and taking annual averages.

Table 1 shows the three basinwide parameters for the world's major rivers at 2° × 2.5° resolution when the local effective flow speed, u, is globally constant at 35 cm s^{-1}. The choice of the value for u is discussed in section 8. The table shows that the basinwide speed, U, is also 35 cm s^{-1}. Also shown are the river lengths weighted by annual precipitation, Λ_{PO} and Λ_{PM}, which are obtained by replacing $\bar{S}$ with $\bar{P}$ in (8); Λ_{PO} is calculated using the observed annual precipitation of Legates and Willmott (1990), and Λ_{PM} uses the GCM's annual precipitation.

It is important to remember that there is no groundwater component to land source runoff and that there is no time delay in surface runoff reaching the rivers and lakes. Thus the flow speed used in Table 1 should be slower than that in the real world, and consequently Ω in Table 1 should also be smaller than that in the real world; Λ and Ω in Table 1 are useful for relative comparisons among the river basins.

TABLE 1. Basinwide parameters from the 2° × 2.5° river routing model with the effective flow speed being globally constant at u = 0.35 m s^{-1}. From left to right the parameters are area (10^{10} m^2), river length weighted by observed and GCM precipitation, Λ_{PO} and Λ_{PM} (km); river length weighted by source runoff, Λ (km); annual turnover rate, Ω (yr^{-1}); and basinwide speed, U (cm s^{-1}). This table shows the relative relationships among different river basins. When groundwater runoff is incorporated into the river routing model, the values of u, Ω, and U will increase.

Area	Λ_{PO}	Λ_{PM}	Λ	Ω	U	River
575	2505	2490	2543	4	35	Amazon
351	2019	2055	2062	5	35	Congo (Zaire)
351	1674	2123	2396	5	35	Mississippi
276	3972	3882	4078	3	35	Nile
271	2144	2328	2245	5	35	Parana (LaPlata)
267	2453	2746	2474	4	35	Yenesei
263	2148	2097	2005	6	35	Ob
236	2242	2203	2115	5	35	Lena
180	2051	2143	2152	5	35	Amur
176	1886	2197	2440	5	35	Yangtze (Changjiang)
157	2198	2209	2176	5	35	Mackenzie
149	1462	1421	1294	9	35	Niger
141	1156	806	733	15	35	Brahmaputra–Ganges
139	1976	1964	2012	5	35	Volga
119	1581	1613	1676	7	35	Zambesi
105	1558	1457	1525	7	35	Tigris–Euphrates
104	1026	955	941	12	35	Orange
104	1265	1263	1211	9	35	Murray
98	1661	1744	1750	6	35	Nelson
95	1497	1417	1323	8	35	Orinoco
92	1538	1767	1852	6	35	Yellow (Huanghe)
86	1131	1320	1711	6	35	Mekong
83	1362	1399	1550	7	35	Danube
83	1542	1584	1691	7	35	Indus
82	1465	1337	1203	9	35	St. Lawrence
77	1279	1365	1480	7	35	Yukon
71	931	1135	1191	9	35	Columbia
69	1045	1107	1147	10	35	Kolyma
65	1322	1155	1092	10	35	Sao Francisco
64	952	996	1024	11	35	Colorado
53	1027	1127	1172	9	35	Rio Grande
44	647	726	774	14	35	Limpopo
44	763	841	970	11	35	Hsi Chiang
35	691	553	520	21	35	Godavari
35	872	980	993	11	35	Indigirka
34	697	676	636	17	35	Severnaya Divina
34	677	825	958	12	35	Irrawady
24	610	590	594	19	35	Rhine
23	584	505	461	24	35	Magdalena
23	520	607	633	17	35	Fraser
15	521	553	585	19	35	Elbe
12	386	399	408	27	35	Loire

The turnover rate Ω is equivalent to a flushing rate that indicates how many times the total river mass is replenished each year. For some idea about the magnitude of Ω, the total annual river flow and river volume of all the world's rivers are approximately 40 000 $km^3\ yr^{-1}$ and 2000 km^3, respectively (Baumgartner and Reichel 1975). This would yield a global turnover rate of 20 yr^{-1}.

The river length weighted by source runoff, Λ, indicates how far from the mouth the source runoff is generated. The reason for including the calculation of

Λ_{PM} is that it can be compared with Λ_{PO}, which can be calculated using the observed precipitation of Legates and Willmott (1990). This comparison gives additional evidence as to whether the model is generating precipitation in the right part of the river basin. Table 1 shows that for most basins, Λ_{PO} and Λ_{PM} are in good agreement. It also shows that for most basins Λ is approximated well by Λ_{PM}.

6. Monthly river flow and topography

Topographic effects are incorporated next. Grid boxes with steeper channel slopes are assumed to flow faster. The downstream gradient, i, of a grid box is calculated as the ratio of the topography difference, Δz, divided by the horizontal distance, d, between a grid box and its downstream neighbor (i.e., $i = \Delta z/d$). Topography is derived from the National Geophysical Data Center (1988) 5-min elevation data. It should be noted that in the calculation of grid-box topography gradients, the slope will be negative if the mean topography of the downstream grid box is at a higher elevation than that of the upstream grid box. In such cases a minimum effective flow speed is specified to assure that water will flow from the grid box. If the minimum is set too low, grid boxes with small or negative topography gradients will act as bottlenecks for the river flow.

Table 2 shows the basinwide parameters when $u = 0.35\ (i/i_0)^{1/2}$, the reference topography gradient is $i_0 = 0.00005$, and u is limited to the range 0.15 to 5 m s^{-1}. An upper limit on u is necessary to prevent numerical instabilities in the river routing model. The choice of the lower limit strongly affects the flow at the mouth, but the choice of the upper limit is less important. Table 2 shows that the turnover rate and basinwide speed change when topography is included. With this formulation for u, the basinwide speed U increases for 30 rivers and decreases for 9 rivers compared with the global constant value of u used in Table 1. The largest increases in Ω and U generally occur in the smaller basins with mountainous terrain.

In addition to the constant speed case with $u = 0.35$ m s^{-1}, two functional forms for the topographic effect on u are examined for the Ob and Sao Francisco Rivers. The functional forms are $u = 0.35\ (i/i_0)^{1/2}$, and $u = 0.35\ i/i_0$, and have lower and upper limits of 0.15 and 5 m s^{-1}, respectively. Table 2 shows that U decreased from the constant speed case for the Ob River and increased for the Sao Francisco River. Figures 6 and 7 show that the principal difference is between the constant case and the case when u has a functional dependence on topography. There is little difference between the square root and linear formulations. Since the Manning formula for channel flow is based on hydraulic principles and assumes that the flow speed is proportional to the square root of the downstream gradient (Linsley et al. 1982), that formulation will be used in the remainder of this paper. For the Ob the inclusion of topography shifts the maximum spring flow at the mouth to later in the year, which is in better agreement with the observations. For the Sao Francisco the inclusion of topography shifts the peak flow at the mouth to earlier in the year, more in agreement with the observed flow and the source runoff.

Figures 8 and 9 show how the minimum effective flow speed affects the monthly flow at the mouths of the Amazon and Amur Rivers when $u = 0.35\ (i/i_0)^{1/2}$. The annual cycle of precipitation is well simulated for each river. The figures show that the timing of the flow at the river mouth is quite sensitive to the

TABLE 2. Basinwide parameters from the 2° × 2.5° river routing model with $u = 0.35\ (i/i_0)^{1/2}$, $i_0 = 0.00005$, $0.15 < u < 5$ m s^{-1}. From left to right the parameters are area, (10^{10} m^2); river length weighted by source runoff, Λ (km); annual turnover rate, Ω (yr^{-1}); and basinwide speed, U (cm s^{-1}). This table shows the relative relationships among different river basins. When groundwater runoff is incorporated into the river routing model, the values of u, Ω, and U will increase.

Area	Λ	Ω	U	River
575	2543	3	25	Amazon
351	2062	6	42	Congo (Zaire)
351	2396	6	46	Mississippi
276	4078	3	35	Nile
271	2245	4	30	Parana (LaPlata)
267	2474	4	29	Yenesei
263	2005	4	25	Ob
236	2115	5	33	Lena
180	2152	5	36	Amur
176	2440	5	39	Yangtze (Changjiang)
157	2176	5	35	Mackenzie
149	1294	10	40	Niger
141	733	24	56	Brahmaputra–Ganges
139	2012	5	35	Volga
119	1676	8	42	Zambesi
105	1525	10	50	Tigris–Euphrates
104	941	37	109	Orange
104	1211	9	33	Murray
98	1750	10	55	Nelson
95	1323	11	44	Orinoco
92	1852	9	55	Yellow (Huanghe)
86	1711	11	59	Mekong
83	1550	8	41	Danube
83	1691	13	69	Indus
82	1203	5	21	St. Lawrence
77	1480	10	47	Yukon
71	1191	9	34	Columbia
69	1147	14	50	Kolyma
65	1092	22	76	Sao Francisco
64	1024	37	119	Colorado
53	1172	39	143	Rio Grande
44	774	52	129	Limpopo
44	970	17	54	Hsi Chiang
35	520	63	104	Godavari
35	993	22	70	Indigirka
34	636	14	29	Severnaya Divina
34	958	17	50	Irrawady
24	594	60	114	Rhine
23	461	30	44	Magdalena
23	633	33	66	Fraser
15	585	37	68	Elbe
12	408	82	106	Loire

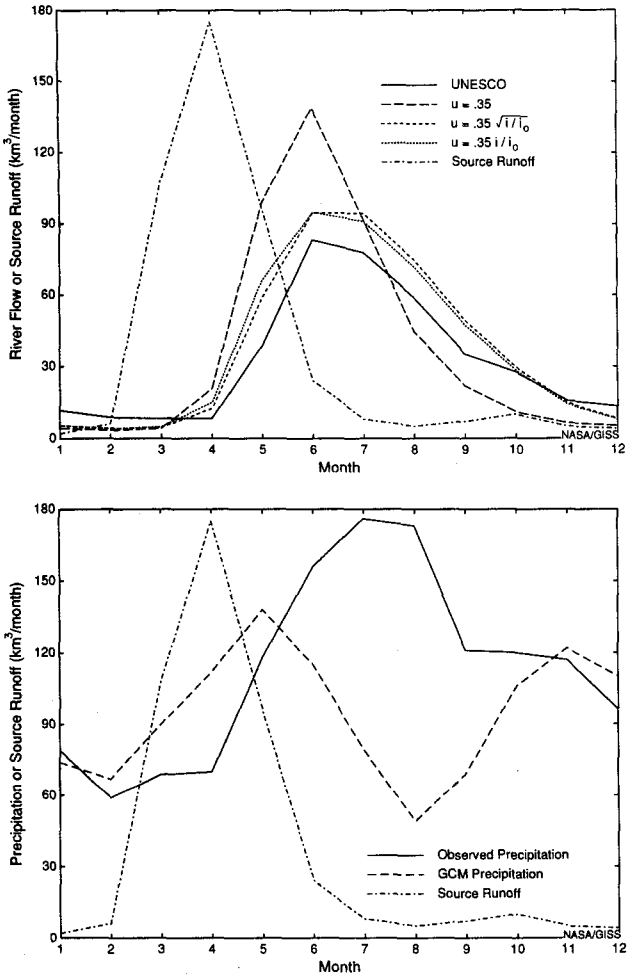

FIG. 6. (a) River flow at the mouth of the Ob River with three different functional forms for the effective flow speed: $u = 0.35$ m s^{-1}, $u = 0.35\ (i/i_0)^{1/2}$, and $u = 0.35\ i/i_0$ where i is the downstream topography gradient, $i_0 = 0.00005$, and $0.15 < u < 5$. The observed river flow is from UNESCO. (b) The monthly basinwide precipitation for the GCM compared with the observations of Legates and Willmott (1990). The source runoff is shown for comparison in both (a) and (b).

choice of the minimum effective flow speed. Low values can produce a bottleneck in the river flow.

7. Grid resolution

The significance of the basinwide parameters defined in section 5 is that they should converge to finite nonzero values as the grid resolution becomes finer. They are therefore useful parameters when comparing model results at different grid resolutions. Table 3 shows the area, the river length weighted by source runoff, the turnover rate, and the basinwide speed derived from the river routing model at 4° × 5° resolution for the case $u = 0.35\ (i/i_0)^{1/2}$. Table 3 should be compared with Table 2, which was derived from the 2° × 2.5° river routing model with the same formulation for u. Comparison of the tables gives an indication of how accurately the basinwide parameters are determined for these resolutions.

Tables 2 and 3 show that for the larger rivers, the basinwide parameters are usually close for the two resolutions. There are discrepancies, however, particularly for the smaller river basins. One reason for this discrepancy is that the smaller river basins are often poorly resolved at the 4° × 5° resolution. Another reason is that the local effective flow speed can vary by an order of magnitude depending on the calculated topography gradient. If this range in the minimum and maximum limits were reduced, the discrepancies would be reduced.

8. Optimizing the flow parameters

In this section, we define a normalized flow error, ϕ, for each river basin as

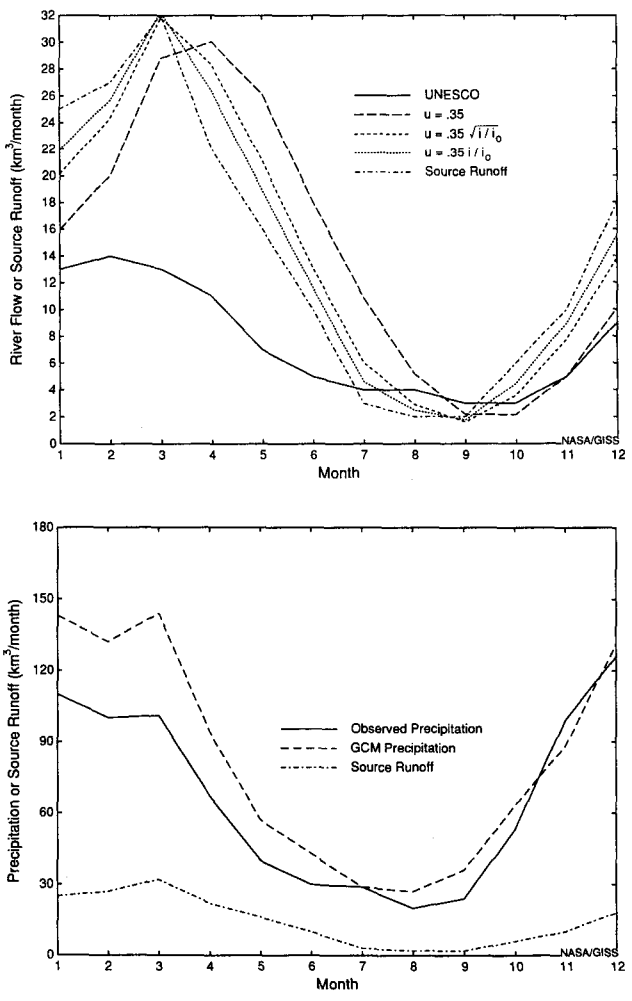

FIG. 7. The Sao Francisco River. Otherwise the same as Fig. 6.

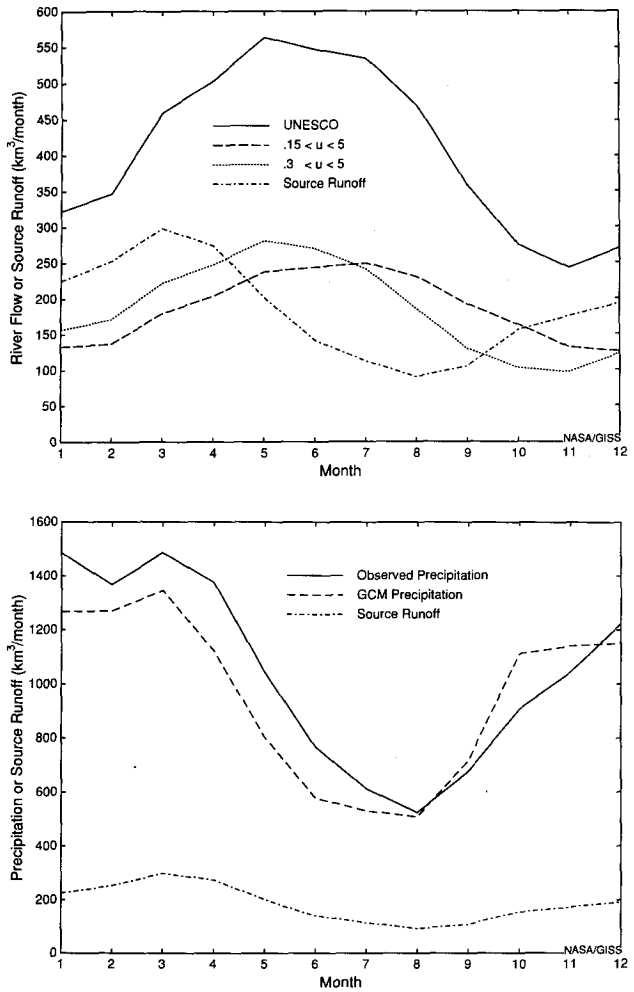

FIG. 8. (a) Flow at the mouth of the Amazon River for two different minimum cutoff values for the effective flow speed where $u = 0.35\ (i/i_0)^{1/2}$. The observed river flow is from UNESCO. (b) The monthly basinwide precipitation for the GCM compared with the observations of Legates and Willmott (1990). The source runoff is shown for comparison in both (a) and (b).

$$\phi = \frac{[\Sigma(F_{\mathrm{MOD}} - F_{\mathrm{OBS}})^2]^{1/2}}{(\Sigma F_{\mathrm{OBS}}^2)^{1/2}}, \qquad (10)$$

where F_{OBS} is the observed climatological monthly river flow near the mouth from UNESCO (1969, 1985), F_{MOD} is the model's river flow near the observation site, and the summations are taken over 12 months. The error, ϕ, is normalized to be zero if the model's monthly flow at the river mouth is identical to the observed and to be unity if the model never has any flow for the given river basin. Large values of ϕ are due to a combination of poor source runoff or poor simulation of river water transport.

One of the difficulties in assessing the accuracy of the river routing model is that precipitation and source runoff are often poorly simulated in the GCM. If the monthly precipitation is poorly simulated for a particular river basin, then one should not expect the monthly river flow at the mouth to be well simulated. For each river, we define a precipitation weighting function, W_P, which is a measure of how well the GCM simulates the annual cycle of precipitation in the river basin, as

$$W_P = 1/(1 + \phi_P)^2, \qquad (11)$$

where ϕ_P is obtained by substituting the GCM and observed monthly precipitation over the basin, P_{MOD} and P_{OBS}, for F_{MOD} and F_{OBS} in (10). If the GCM and observed precipitation are the same each month, then $W_P = 1$. Otherwise W_P is less than one, and if the GCM precipitation were zero each month, then $W_P = 0.25$. The first column of Table 4 shows W_P for river basins for which observed monthly river flow near the mouth is available. One should note that W_P indicates how well the GCM simulates the monthly precipitation in the river basin but does not provide information on whether the precipitation is occurring in the right part

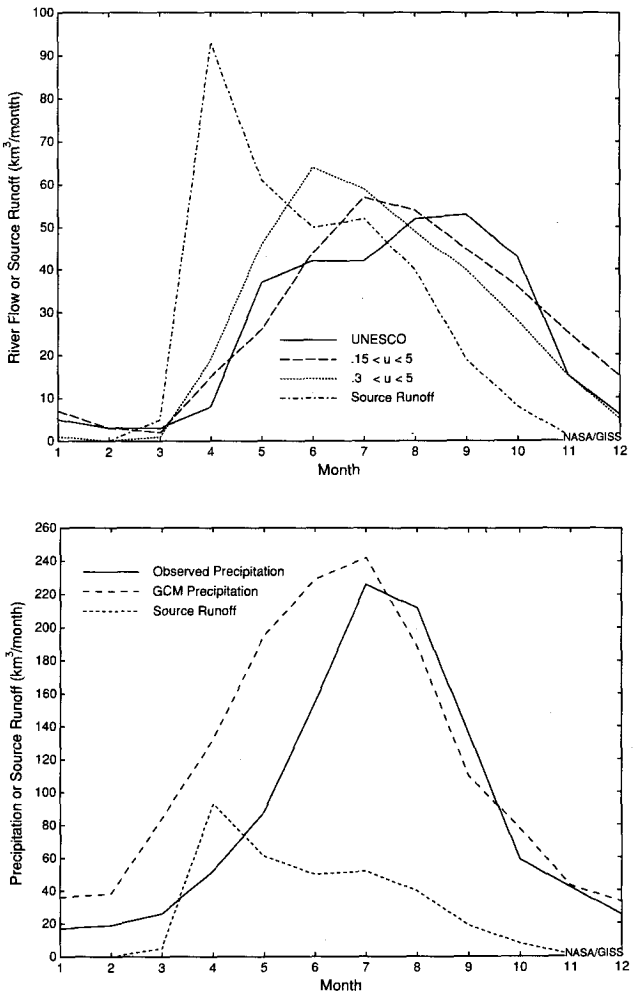

FIG. 9. The Amur River. Otherwise the same as Fig. 8.

TABLE 3. Basinwide parameters from the 4° × 5° river routing model with $u = 0.35\,(i/i_0)^{1/2}$, $i_0 = 0.00005$, $0.15 < u < 5$ m s^{-1}. From left to right the parameters are area, (10^{10} m^2); river length weighted by source runoff, Λ (km); annual turnover rate, Ω (yr^{-1}); and basinwide speed, U (cm s^{-1}). This table shows the relative relationships among different river basins. When groundwater runoff is incorporated into the river routing model, the values of u, Ω, and U will increase.

Area	Λ	Ω	U	River
629	2575	3	27	Amazon
363	2482	7	56	Congo (Zaire)
349	2660	5	42	Mississippi
291	3295	6	58	Nile
303	2083	7	46	Parana (LaPlata)
255	2192	5	38	Yenesei
291	2327	4	26	Ob
244	2112	4	28	Lena
200	1544	9	44	Amur
214	2173	16	109	Yangtze (Changjiang)
163	1688	7	39	Mackenzie
189	1467	8	36	Niger
170	889	51	143	Brahmaputra–Ganges
172	2088	5	31	Volga
124	1532	13	62	Zambesi
103	1499	6	29	Tigris–Euphrates
98	1285	33	136	Orange
87	1178	18	66	Murray
139	1500	18	87	Nelson
84	1149	23	83	Orinoco
116	2136	14	94	Yellow (Huanghe)
95	1054	30	100	Mekong
91	1187	11	42	Danube
104	1741	6	36	Indus
101	1016	6	20	St. Lawrence
82	1520	18	87	Yukon
64	914	61	176	Columbia
69	966	18	55	Kolyma
66	1141	28	103	Sao Francisco
62	1225	49	190	Colorado
53	1444	25	113	Rio Grande
37	941	47	141	Limpopo
52	450	77	110	Hsi Chiang
63	499	77	122	Godavari
42	921	27	79	Indigirka
48	551	22	38	Severnaya Divina
75	1113	42	148	Irrawady
17	529	66	111	Rhine
19	444	106	149	Magdalena
33	513	75	122	Fraser
7	543	15	26	Elbe
23	336	138	147	Loire

of the basin. This deficiency could be corrected by summing over all grid boxes in the basin as well as over months in calculating ϕ_P.

A global error of river flow can now be defined that is a measure of how well the climate model represents river flow at the mouths of the rivers in Table 4. The precipitation weighting function is used to give greater weight to river basins in which the precipitation is well simulated by the model. The global error of river flow, Φ, is defined as

$$\Phi = \frac{\Sigma\{W_P[\Sigma(F_{\mathrm{MOD}} - F_{\mathrm{OBS}})^2]^{1/2}\}}{\Sigma[W_P(\Sigma F_{\mathrm{OBS}}^2)^{1/2}]}, \qquad (12)$$

where for both numerator and denominator the outside summations are over the river basins and the inside summations are over the 12 months. If the model's monthly river flow is the same as the observed for each river, then $\Phi = 0$. If the model's monthly river flow is zero for each river, then $\Phi = 1$. The error formulation in (10) and (12) is similar to that of Nash and Sutcliffe (1970).

Figure 10 shows how Φ depends on different values of globally constant u. The solid line is for the case in which the river routing model uses the GCM's land source runoff that does not contain a groundwater component. The globally constant value of $u = 0.35$ m s^{-1} was used in section 5 because it minimizes Φ at 0.58. The second column of Table 4 shows the flow error ϕ when the river routing model is run with the optimized global constant $u = 0.35$. The third column of Table 4 shows the error when u depends on the topography gradient and is given by $u = 0.35\,(i/i_0)^{1/2}$ where $i_0 = 0.00005$ and $0.15 < u < 5$. The lower limit of 0.15 m s^{-1} is used in section 6 because it gave the minimum value of $\Phi = 0.566$ when the river routing model was run with several different minimum speeds.

One purpose of this paper is to determine whether the river routing model described here is a better way to calculate river flow at the mouth than by moving the source runoff to the mouth instantaneously or by using the mean annual value of the flow at the mouth. If u were infinite, which means that all source runoff would reach the river mouth instantaneously, then $\Phi = 0.78$, which does not compare favorably with $\Phi = 0.58$ when $u = 0.35$ nor with $\Phi = 0.566$ when $u = 0.35\,(i/i_0)^{1/2}$. The routing model is thus an improvement over assuming that all source runoff reaches the river mouth instantaneously. It is less clear that the routing model is a significant improvement over using the mean annual flow for the monthly flow at the mouth, as Φ then converges to 0.60.

It is important to note that the source runoff in this paper is based on a GCM and not observations. It is also important to note that the value of u for which the minimum Φ is attained for the solid line in Fig. 10 is based on neglect of groundwater runoff as discussed in section 2. The sensitivity of the results to including groundwater runoff can be examined by allowing a portion of the land source runoff to be delayed in reaching the rivers. The dotted line of Fig. 10 shows how Φ depends on the global constant u when half the land source runoff is apportioned to groundwater runoff in each grid box with one-thirtieth of this groundwater reservoir reaching the river each day. The other half, which is surface runoff, is still assumed to reach the river channel during the same time step in which it is generated. As expected, the optimal value of u increases to 0.5 m s^{-1}, and the minimum value of Φ is 0.57. The flow errors for this case are shown in the fourth column of Table 4. The fifth column of Table 4 is obtained by running the river routing model with

TABLE 4. Column 1 is the precipitation weighting function defined by (11). Columns 2 and 3 are the normalized flow errors ϕ defined by (10) from the 2° × 2.5° river routing model without groundwater runoff for two cases: $u = 0.35$ m s^{-1} and $u = 0.35\,(i/i_0)^{1/2}$, $i_0 = 0.00005$, $0.15 < u < 5$. Columns 4 and 5 are the normalized flow errors from the river routing model with groundwater runoff for two cases: $u = 0.5$ m s^{-1} and $u = 0.5\,(i/i_0)^{1/2}$, $i_0 = 0.00005$, $0.2 < u < 5$.

	No groundwater runoff		With groundwater runoff		
W_P	$u = .35$	$.35(i/i_0)^{1/2}$	$u = .5$	$.5(i/i_0)^{1/2}$	River
0.764	0.538	0.553	0.541	0.544	Amazon
0.522	0.241	0.229	0.244	0.235	Congo (Zaire)
0.585	0.894	0.812	0.861	0.790	Mississippi
0.304	4.891	4.855	4.886	4.856	Nile
0.611	0.284	0.241	0.287	0.253	Parana (LaPlata)
0.437	0.577	0.656	0.455	0.571	Yenesei
0.486	0.620	0.257	0.684	0.334	Ob
0.338	0.564	0.536	0.460	0.478	Lena
0.487	0.270	0.232	0.244	0.214	Amur
0.400	0.568	0.532	0.544	0.526	Yangtze (Changjiang)
0.274	1.225	1.123	1.243	1.162	Mackenzie
0.529	0.283	0.295	0.291	0.317	Volga
0.727	1.410	1.332	1.387	1.323	Zambesi
0.496	0.513	0.477	0.517	0.491	Orinoco
0.402	0.730	0.761	0.730	0.752	Mekong
0.549	0.279	0.253	0.273	0.255	Danube
0.628	0.443	0.348	0.439	0.372	St. Lawrence
0.233	1.340	1.309	1.301	1.283	Yukon
0.428	0.630	0.604	0.611	0.569	Columbia
0.204	4.075	4.237	3.968	3.998	Kolyma
0.606	1.416	1.386	1.362	1.327	Sao Francisco
0.207	25.426	26.119	24.889	25.151	Rio Grande
0.451	2.643	2.815	2.574	2.656	Limpopo
0.420	0.730	0.717	0.752	0.737	Godavari
0.177	1.832	2.083	1.708	1.811	Indigirka
0.654	0.539	0.472	0.418	0.367	Severnaya Dvina
0.417	0.765	0.779	0.749	0.750	Rhine
0.339	0.466	0.465	0.466	0.465	Magdalena
0.365	1.033	1.085	0.971	0.997	Fraser
0.482	1.610	1.631	1.595	1.602	Elbe
0.343	1.378	1.368	1.388	1.376	Loire
Φ	0.581	0.566	0.570	0.558	

$u = 0.5\,(i/i_0)^{1/2}$, $i_0 = 0.00005$, $0.2 < u < 5$, and with half of the land source runoff coming from groundwater runoff. The lower limit of 0.2 m s^{-1} gave the minimum value of $\Phi = 0.558$ when the river routing model was run with several different lower-limit speeds.

9. Discussion and summary

The river routing model introduced here provides a basis for closing the hydrologic cycle in a coupled atmosphere–ocean model. Within a continental grid box, precipitation or snowmelt can run off into a river system and then continue to move downstream until it enters the ocean as a freshwater source. The GCM first calculates how much water runs off into the river within a continental grid box. The direction of flow from a grid box is then determined from direction files compiled for 4° × 5° and 2° × 2.5° resolutions. The speed of flow is either constant or depends on the topography gradient. The river flow at the mouth is compared with observations, which provides a good diagnostic for evaluating the ability of a GCM to simulate precipitation, snowmelt, and land–atmosphere interactions.

The magnitude and timing of river flow at the mouth depend on many factors. Among these are the distribution of precipitation within a river basin, the timing of snowmelt, the evaporation rate, the time it takes for surface and groundwater runoff to reach the river channel, and the rate at which water is transported downstream. If the monthly precipitation and evaporation are simulated poorly, then the river flow calculations are not very useful. If the precipitation and evaporation are simulated well, then the flow at the river mouth depends on how water moves within individual grid boxes and how it flows downstream to subsequent grid boxes.

For high-latitude rivers, snowmelt is the major contributor to source runoff in the spring. The GCM's ability to accumulate snow during the winter and to obtain the correct surface temperature is critical for reproducing the proper magnitude and timing of the spring snowmelt. The hydrology model's ability to

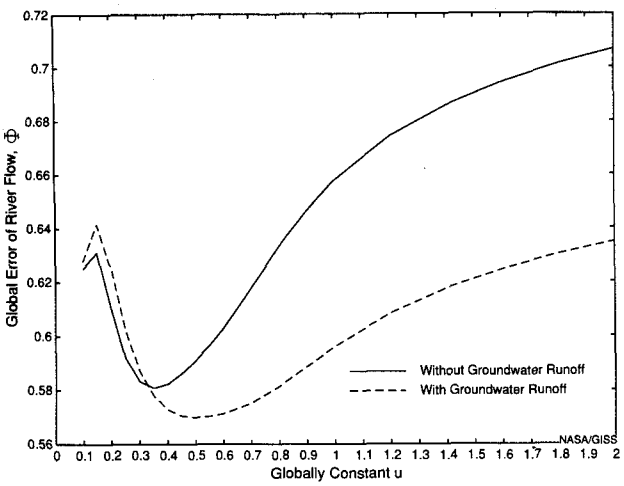

FIG. 10. Global error of river flow, Φ, without and with groundwater runoff. As u approaches infinity, Φ converges to 0.78 in the case without groundwater runoff. As u approaches zero, Φ converges to 0.60 for both cases.

move water into the river channel and the routing model's ability to transport water downstream are critical for reproducing the proper magnitude and timing of the maximum discharge at the river mouth in the spring.

Within grid boxes, there is still much work to be done to determine the magnitude and timing of runoff into rivers. Hydrologists and climate modelers must develop better parameterizations of land–atmosphere interactions within GCMs to improve the calculation of grid-box source runoff. The two-layer water storage model used in this simulation does not include a groundwater component. A more physically based six-layer model that does include groundwater has been developed by Abramopoulos et al. (1988) and will be incorporated into future versions of the GCM. Probst and Sigha (1989) have calculated the contribution of surface runoff to river flow for 26 of the world's major rivers, and their results could be used to divide the GCMs' land source runoff into surface and groundwater components.

In this paper, the rate at which water moves downstream is assumed to depend on the mass of water stored above the sill depth in rivers or lakes, the effective flow speed u leaving each grid box, and the downstream distance between grid boxes. The timing of flow at the river mouth is sensitive to whether u is a global constant or has a topography gradient dependence and also is sensitive to the minimum speed if there is a topography gradient dependence. The timing is less sensitive to whether the square root or linear dependence on the topography gradient is used. The effective flow speed should include a dependence upon the river surface gradient, and not simply upon the downstream topography gradient as was used in this paper.

More work is needed to improve the functional form for river flow used in (4). Liston et al. (1994) have applied a river routing scheme with a more complex formulation to the Mississippi River. As a way to determine how well different formulations work, a global error of river flow Φ has been defined. It is based on monthly river flow at the river mouth and includes a precipitation weighting function that gives greater weight to river basins for which the monthly precipitation is well simulated. One option is to define u locally for each river basin or for each grid box in order to minimize the flow error ϕ for each river basin. A more satisfying approach is to minimize the global error Φ by basing the effective flow speed u on global physical principles that might include such hydrologic factors as downstream slope, channel cross-sectional area, bottom friction, or the mass of water in the river.

Two characteristic parameters of river basins are their area and annual discharge at the mouth. In this paper, three additional basinwide parameters are described: the river length weighted by source runoff, the turnover rate, and the speed. These basinwide parameters converge as the grid resolution becomes finer. One reason for the discrepancies between the parameters for the two tested resolutions is that the smaller rivers are poorly resolved for the 4° × 5° resolution. As GCMs simulate physical processes better and as their resolutions become finer, these basinwide parameters will be defined more accurately. It is important to note that the basinwide parameters in Table 1–3 are based on GCM source runoff, which had no groundwater component.

When climate models are able to simulate river flow for the present climate more accurately, they can then be used to examine potential changes in response to climate change. They also could be used to examine transport of heat, sediment, and chemical species within river systems. Precipitation and temperature fields from GCMs have been used in hydrologic models to predict regional changes in river flow that would accompany future global warming (Gleick 1987; Lettenmaier and Gan 1990). Miller and Russell (1992) have used the GCM of Hansen et al. (1983) to calculate potential changes in annual river discharge using the land source runoff generated by the GCM. This land source runoff can now be used with the river direction file and the river routing model to improve the seasonal cycle of river flow in global climate models and to examine potential changes in river flow in future climates.

Acknowledgments. We would like to thank J. Hanson for helping to prepare the figures, and B. Oppenheimer for helping to define the river basins.

REFERENCES

Abramopoulos, F., C. Rosenzweig, and B. Choudhury, 1988: Improved ground hydrology calculations for global climate models (GCMs): Soil water movement and evapotranspiration. *J. Climate,* **1**, 921–941.

Baumgartner, A., and E. Reichel, 1975: *The World Water Balance.* Elsevier, 178 pp.

Entekhabi, D., and P. S. Eagleson, 1989: Land surface hydrology parameterization for atmospheric general circulation models including subgrid scale spatial variability. *J. Climate,* **2,** 816–831.

Gleick, P. H., 1987: Regional hydrological consequences of increases in atmospheric CO_2 and other trace gases. *Clim. Change,* **10,** 137–160.

Hansen, J., G. Russell, D. Rind, P. Stone, A. Lacis, S. Lebedeff, R. Ruedy, and L. Travis, 1983: Efficient three-dimensional global models for climate studies: Models I and II. *Mon. Wea. Rev.,* **111,** 609–662.

Korzoun, V. I., A. A. Sokolov, M. I. Budyko, K. P. Voskresensky, G. P. Kalinin, A. A. Konoplyantsev, E. S. Korotkevich, and M. I. Lvovich, Eds., 1977: *Atlas of World Water Balance.* USSR National Committee for the International Hydrological Decade, UNESCO Press.

Kuhl, S. C., and J. R. Miller, 1992: Seasonal river runoff calculated from a global atmospheric model. *Water Resour. Res.,* **28,** 2029–2039.

Legates, D., and C. Willmott, 1990: Mean seasonal and spatial variability in gauge-corrected global precipitation. *Int. J. Climatol.,* **10,** 111–127.

Lettenmaier, D. P., and T. Y. Gan, 1990: Hydrologic sensitivities of the Sacramento–San Joaquin River Basin, California, to global warming. *Water Resour. Res.,* **26,** 69–86.

Linsley, R. K., M. A. Kohler, and J. L. H. Paulhus, 1982: *Hydrology for Engineers.* McGraw-Hill, 508 pp.

Liston, G. E., Y. C. Sud, and E. F. Wood, 1994: Evaluating GCM land surface hydrology parameterizations by computing river discharges using a runoff routing model: Application to the Mississippi Basin. *J. Appl. Meteor.,* **33,** 394–405.

Matthews, E., 1983: Global vegetation and land use: New high-resolution data bases for climate studies. *J. Climate Appl. Meteor.,* **22,** 474–487.

Miller, J. R., and G. L. Russell, 1992: The impact of global warming on river runoff. *J. Geophys. Res.,* **97,** 2757–2764.

Milliman, J. D., and R. H. Meade, 1983: World-wide delivery of river sediment to the oceans. *J. Geology,* **91,** 1–21.

Mysak, L. A., D. K. Manak, and R. F. Marsden, 1990: Sea-ice anomalies observed in the Greenland and Labrador Seas during 1901–1984 and relation to an interdecadal Arctic climate cycle. *Climate Dyn.,* **5,** 111–133.

Nash, J. E., and J. V. Sutcliffe, 1970: River flow forecasting through conceptual models. Part I—A discussion of principles. *J. Hydrol.,* **10,** 282–290.

National Geophysical Data Center, 1988: Digital relief of the surface of the Earth (ETOPO5). Data Announcement 88-MGG-02, U.S. Dept. Commerce.

Probst, J.-L., and N. Sigha, 1989: Estimation of the surface runoff and its suspended load in some major world river basins. *C. R. Acad. Sci. Paris,* **309,** 357–363.

Russell, G., and J. R. Miller, 1990: Global river runoff calculated from a global atmospheric general circulation model. *J. Hydrol.,* **117,** 241–254.

Singh, V. P., 1989: *Hydrologic Systems.* Vol. II. Watershed Modeling. Prentice Hall, 320 pp.

The Times of London, 1967. *Times Atlas of the World.* John Bartholomew and Son Ltd.

UNESCO, 1969: *Discharge of Selected Rivers of the World.* Vol. 1. *General and Regime Characteristics of Stations Selected.* UNESCO Press, 70 pp.

——, 1985: *Discharge of Selected Rivers of the World.* Vol. 3. Part 4. *Mean Monthly and Extreme Discharges (1976–1979).* UNESCO Press, 126 pp.

Van Blarcum, S. C., 1992: Modeling present and future river runoff using global atmospheric models. M.S. thesis, Graduate Program in Meteorology, Rutgers University, 117 pp. [Available from Department of Meteorology, P.O. Box 231, Cook College, Rutgers University, New Brunswick, NJ 08903.]

Vorosmarty, C. J., B. Moore, A. L. Grace, M. P. Gildea, J. M. Melillo, B. J. Peterson, E. B. Rastetter, and P. A. Steudler, 1989: Continental scale models of water balance and fluvial transport: An application to South America. *Global Biogeochem. Cycles,* **3,** 241–265.

Wood, E. F., D. P. Lettenmaier, and V. G. Zartarian, 1992: A land surface hydrology parameterization with sub-grid variability for general circulation models. *J. Geophys. Res.,* **97,** 2717–2728.